Title

Photoreactivity of a Quantum Dot–Ruthenium Nitrosyl Conjugate

Journal

The Journal of Physical Chemistry A, 118(51)

ISSN

1089-5639

Authors

Franco, Lilian Pereira
Cicillini, Simone Aparecida
Biazzotto, Juliana Cristina
et al.

Publication Date

2014-12-26

DOI

10.1021/jp5111218

Peer reviewed

THE JOURNAL OF PHYSICAL CHEMISTRY A

Article

pubs.acs.org/JPCA

Photoreactivity of a Quantum Dot−Ruthenium Nitrosyl Conjugate

Lilian Pereira Franco,[†] Simone Aparecida Cicillini,[†] Juliana Cristina Biazzotto,[†] Marco A. Schiavon,[‡] Alexander Mikhailovsky,[§] Peter Burks,[§] John Garcia,[§] Peter C. Ford,*[,§] and Roberto Santana da Silva*[,†]

[†]Faculdade de Ciências Farmacêuticas de Ribeirão Preto, University of Sao Paulo, Avenida do Café s/n, 14040-903 Ribeirão Preto, Sao Paulo, Brazil

[‡]Departamento de Ciências Naturais, Universidade Federal de São João Del Rei, Campus Dom Bosco, Praça Dom Helvécio, 74, 36301-160 São João Del Rei, Minas Gerais, Brazil

[§]Department of Chemistry and Biochemistry, University of California, Santa Barbara, California 93110-9510, United States

Supporting Information

ABSTRACT: We describe the use of cadmium telluride quantum dots (CdTe QDs) as antennas for the photosensitization of nitric oxide release from a ruthenium nitrosyl complex with visible light excitation. The CdTe QDs were capped with mercaptopropionic acid to make them water-soluble, and the ruthenium nitrosyl complex was *cis*-$[Ru(NO)(4\text{-ampy})(bpy)_2]^{3+}$ (Ru−NO; bpy is 2,2′-bipyridine, and 4-ampy is 4-aminopyridine). Solutions of these two components demonstrated concentration-dependent quenching of the QD photoluminescence (PL) as well as photoinduced release of NO from Ru−NO when irradiated by 530 nm light. A NO release enhancement of ∼8 times resulting from this association was observed under longer wavelength excitation in visible light range. The dynamics of the quenching determined by both PL and transient absorption measurements were probed by ultrafast flash photolysis. A charge transfer mechanism is proposed to explain the quenching of the QD excited states as well as the photosensitized release of NO from Ru−NO.

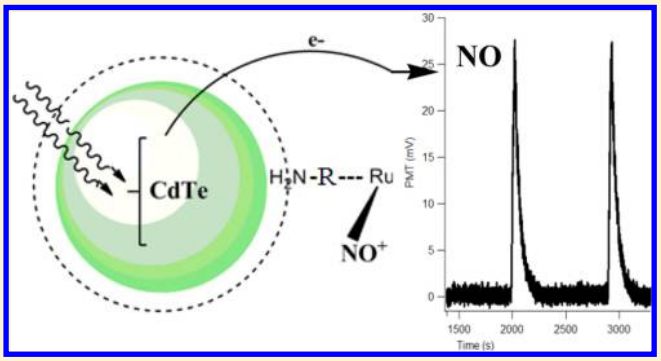

INTRODUCTION

Quantum dots (QDs) have attracted considerable attention as photoactive components in functional materials owing to their uniquely shape- and size-dependent optical properties including strong absorption, high photoluminescence (PL), and surfaces that can be customized by ligand exchange.[1−4] Such characteristics are particularly useful in light-harvesting systems, as these nanoparticles could generate photocurrent under light irradiation, which is dependent on the band gap energies. The charge accumulation could also conduct to vectorial charge transfer for different applications. CdTe is a promised semiconductor toward to development of higher power conversion efficiency QDs solar cells (QDSC).[5] Functional ligands on a QD surface can improve photoelectrochemical properties of QDs as well as act as binders to uncoordinated molecules as metal complexes.[6] In this way, QDs have been proposed as sensitizers for biological applications including photodynamic therapy[7] and photoactivated drug delivery since the photochemical reaction as well as the dosage of drug can be controlled by light.[8−10] These unique properties could make QDs useful in prodrug activation systems that release biologically relevant molecules by external stimulation. Our group has been working with photoinduced systems focusing on nitric oxide release.[11,12] Ruthenium nitrosyl complexes are stable NO donors that can be designed to deliver NO at defined rates when activated by reduction and/or by light irradiation.[13−16] Besides the physiological functions of NO, such as vasorelaxation and tumoricidal activities, the NO concentration has to be controlled due to its toxicity at higher levels. In the present work, our interest has focused on the construction of conjugates between QDs and coordination compounds that might serve as photochemical precursors for delivering bioactive substances to physiological targets. In this context, we describe a photoactive conjugate formed between the ruthenium nitrosyl complex *cis*-$[Ru(NO)(4\text{-ampy})(bpy)_2](PF_6)_3$ (Ru−NO; bpy is 2,2′-bipyridine, and 4-ampy is 4-aminopyridine) and cadmium telluride quantum dots that have been made water-soluble by capping the surface with mercaptopropionic acid. This CdTe QD···Ru−NO conjugate shows promise as a visible light activated prodrug for the targeted release of NO. In addition, the QD luminescence may allow tracking of the location of the NO delivery conjugate in cellular systems.

EXPERIMENTAL SECTION

Chemical Reagents. Cadmium chloride hydrate ($CdCl_2 \cdot 2H_2O$) was obtained from Merck. Sodium borohydride

Received: November 17, 2014
Published: November 18, 2014

   dx.doi.org/10.1021/jp5111218 | J. Phys. Chem. A 2014, 118, 12184−12191

($NaBH_4$, 99%), tellurium powder, and 3-mercaptopropionic acid (MPA, 99%) were purchased from Aldrich. All chemicals were used without further purification. Distilled water was used throughout.

Apparatus. Electronic absorption spectra were recorded on a Shimadzu dual beam UV-2401 PC spectrophotometer or a Hitachi U-3501 spectrophotometer. Photoluminescence spectra were recorded using a Photon Technology International (PTI) fluorimeter at 1 nm resolution with a model 814 PMT detector or model RF-5301PC Shimadzu spectrofluorimeter. Optical studies were performed in 1 cm path length quartz cells. A Digimed model DM-20 pH meter was used for pH measurements. An Atto electrophoresis chamber apparatus (Model AE6500) was used for electrophoresis experiments. Infrared spectra were recorded on a PerkinElmer Spectrum Two UATR FT-IR spectrometer.

Quantum dot luminescence lifetime measurements were performed at the UCSB Optical Characterization Facility (OCF) using the time-correlated single photon counting (TCSPC) technique.[17] Excitation pulses at 400 nm, 200 fs were generated with a Ti:sapphire laser (Coherent Mira 900) with the laser repetition rate reduced to 1 MHz by a custom-built acoustooptical pulse picker in order to avoid saturation of the chromophore. The TCSPC system is equipped with an ultrafast microchannel plate photomultiplier tube detector (Hamamatsu R3809U-51) and electronics board (Becker & Hickl SPC-630) and has an instrument response time of about 60−65 ps. The fluorescence signal was dispersed in an Acton Research SPC-500 monochromator after passing through a pump blocking, long-wavelength-pass, autofluorescence-free, interference filter (Omega Filters, ALP series). The monochromator is equipped with a CCD camera (Roper Scientific PIXIS-400) allowing for monitoring of the time-averaged fluorescence spectrum. The instrument response for PL experiments was ∼70 ps.

Transient absorption (TA) measurements were also performed at the OCF using a custom-built setup similar to one described previously.[18] The output of a Ti:sapphire regenerative amplifier (Spectraphysics Spitfire, 800 nm, 120 fs, 1 mJ pulses with 1 kHz repetition rate) was divided with a 10/80 ratio into probe and pump beams, respectively. The samples for TA spectroscopy were placed into quartz cells with optical path lengths of 1 mm. The optical density of the solution at 400 nm was adjusted to 0.1. In order to avoid effects such as multiexciton Auger-type recombination,[19] TA transients were acquired at several, gradually reduced levels of the excitation pulse energy until pump-dependent components of the TA signal disappeared. The excitation wavelengths were 370 and 400 nm.

Synthesis and Characterization of the Nitrosyl Ruthenium Complex *cis*-[Ru(bpy)$_2$(4ampy)(NO)](PF$_6$)$_3$. This compound was prepared by the procedure reported by Ershov and Col with some modifications.[20,21] A 0.100 g sample of the precursor [Ru(NO$_2$)(4-ampy)(bpy)$_2$](PF$_6$) was dissolved in 20.0 mL of anhydrous acetonitrile, and 1.0 mL of concentrated HPF_6 was then added to this solution. After 15 min of reaction, the solution was filtered and concentrated under vacuum. Then, 2.0 mL of distilled water was added, and the reddish-orange solid *cis*-[Ru(NO)(4-ampy)(bpy)$_2$](PF$_6$)$_3$ precipitated. After refrigeration for 1 h, this was collected by filtration, washed with ether, and placed in a desiccator for 24 h. Yield, 78.0%. Purification was performed by recrystallization from acetonitrile and drying the resulting solid under vacuum. The obtained solid was characterized by electronic, infrared (ATR-IR) spectroscopy and elemental analysis. The formation of the nitrosyl ligand was evidenced by appearance of a strong band at 1939 cm^{-1} in the infrared spectrum of the resulting solid as described in the literature.[20,21] Elem. anal. Calcd for *cis*-[Ru(NO)(4-ampy)(bpy)$_2$](PF$_6$)$_3$.H$_2$O: C, 30.86; N, 10.10; H, 2.22. Found: C, 30.31; N, 9.90; H, 2.44.

Synthesis and Characterization of MPA-Capped CdTe QDs. The water-soluble MPA-CdTe QDs were prepared by the method described by Li et al.[22] with some modifications using 3-mercaptopropionic acid as stabilizer agent. The MPA-CdTe QDs were obtained after the reaction in water of MPA, $CdCl_2$, and NaHTe for 3 h in the proportions Cd:Te:MPA = 1:0.2:2.4.

A freshly prepared NaHTe solution (0.78 mmol of Te and 0.64 mmol of $NaHB_4$) was injected into the three necked flask containing the solution of $CdCl_2{\cdot}H_2O$ (0.40 mmol) and MPA (1.7 mmol) under an argon atmosphere, and the reaction was allowed to proceed for 3 h at 100 °C. After this, a red-brown solid was obtained by adding acetone in excess, followed by centrifugation.[23] The resulting solid was characterized by electronic and PL spectroscopy (Supporting Information (SI) Figure S-1). The size distribution of the MPA-CdTe QDs were determined by transmission electron microscopy (TEM) on a TEM Tecnai G2 F-20 S transmission electron microscope.

Photochemical and Photophysical Studies. The emission quantum yields (QY) of MPA-CdTe QD samples were determined by the ratio method (eq 1)[24−26] using rhodamine B (QY = 0.7 in ethanol) as the standard. Q_R, OD_R, and n_R are the QY, absorbance, and solvent refraction of the reference solution.

$$QY = Q_R \frac{I}{I_R} \frac{OD_R}{OD} \frac{n}{n_R} \quad (1)$$

Interactions between the MPA-CdTe QDs and Ru−NO were probed by preparing aqueous solutions of both compounds in different concentrations. Quenching experiments were carried out with aqueous or citrate buffered stock solutions of the QDs (exciton absorbance around ∼0.30 and of the quencher *cis*-[Ru(NO)(4-ampy)(bpy)$_2$](PF$_6$)$_3$ (0.6 μM) freshly prepared on the same day. The experiment was done by adding a 100 μL aliquot of the QD stock solution in water into 2.9 mL aqueous samples with various Ru−NO concentrations contained in a 1.0 cm quartz cuvette. This 30-fold dilution gave a final QD concentration around 100 nM. Emission spectra (λ_{ex} = 320 and 460 nm) were then recorded for these solutions at different complex concentrations. Reported PL intensities were corrected for modest inner filter effects due to quencher absorption (ruthenium species) of excitation light and of the QD emission. This was done by assuming an average path length of 0.5 cm (PL detection was at 90°), converting the quencher absorption at the specified wavelength to transmittance, and then correcting the QD PL intensity accordingly.[27]

NO photorelease was evaluated using two methods. The first used laser diode (Colibri QuantumTech) irradiation at 532 nm for photoexcitation and a nitric oxide selective electrode amiNO-700, Innovative Instruments, Inc. The cuvette was partially covered to ensure the electrode was not directly illuminated. The second method used a General Electric model NOA-280i nitric oxide analyzer (NOA) under a flow of helium to analyze the NO generated. The sensitivity of the first method is from 1 nM to 20 μM while the second is 1 pmol (1 nM in 1

dx.doi.org/10.1021/jp5111218 | J. Phys. Chem. A 2014, 118, 12184−12191

mL) to micromoles (mM concentration in the liquid sample). The experimental procedures were carried out using buffered solutions of Ru−NO alone and the same solutions after addition of a 100 μL sample of QD stock solution. Using the latter method, the photolysis quantum yield was determined from the NO released using the integrated NOA signal, the Einsteins of photons absorbed, and the irradiation time. The absorption spectra were recorded before and after photolysis.

Analysis of the Interaction between Compounds by Electrophoresis. In an electrophoresis chamber, agarose gel (1%) prepared without addition of ethidium bromide was submerged in running buffer solution 1X TAE (Tris-acetate: 40 mM Tris, 20 mM acetic acid (Ac), and 1 mM ethylenediaminetetraacetic acid (EDTA)). Samples containing only QDs (MPA-CdTe) or mixtures of QDs and quencher at different concentrations were applied to each well after adding 4 μL aqueous solution of 30.0% glycerin (w/v).[28] The run was performed at 90 V for 20−50 min, and then the gel bands were observed under ultraviolet light.

Superoxide Anion Production. Superoxide anion production was evaluated by electron-paramagnetic resonance spectroscopy using a JEOL electron paramagnetic resonance (EPR) spectrometer model JES-FA 200 and the radical 2,2,6,6-tetramethylpiperidine-1-oxyl (TEMPO) as a spin trap. The instrument settings were as follows: microwave power, 10 mW; modulation amplitude, 100; time constant, 0.3 s, scan time, 1 min. Aqueous QD solutions were under irradiation for different periods of time, and the production of free radicals was studied following the changes in spin-trap signal versus time. The measurements were performed with the QD aqueous solution under irradiation at 532 nm in different time intervals using a nonirradiated solution as control. The samples were placed in quartz capillaries with the same volumes.

RESULTS AND DISCUSSION

The motivation of this work was to probe the potential use of quantum dots as antennae for photoinduced NO delivery from nitrosyl−ruthenium complexes. First, we will discuss the interaction between the water-soluble anionic MPA-CdTe QDs and the cationic complex Ru−NO.

Photophysical Studies. The electronic absorption data of Ru−NO displays two bands at 252 and 296 nm and a shoulder at 332 nm (Figure 1). The complex shows no luminescence in ambient temperature solutions.

The CdTe QDs used here were capped with the hydrophilic ligand mercaptopropionic acid, which makes them water-soluble and protects them from agglomeration.[29] In aqueous solution, these MPA-CdTe QDs displayed an exciton absorption band at λ_{max} = 503 nm (Figure 1) and a photoluminescence (PL) band at λ_{max} = 546 nm with a full width at half-maximum (fwhm) of 50 nm (at λ_{ex} = 320 nm; see SI Figure S-1). According to the empirical relationship proposed by Yu et al.[30] (eq 2) relating the QD diameter D to the wavelength (λ) of the first absorption peak (503 nm), the average particle diameter was estimated as ∼2.4 ± 0.21 nm for the MPA-capped CdTe used here, and this was confirmed by TEM experiments. On this basis, the coefficient of molar absorptivity (ε) calculated for these MPA-CdTe QDs is ∼6.6 × 10^4 M^{-1} cm^{-1}.

$$D = (9.8127 \times 10^{-7})\lambda^3 - (1.7147 \times 10^{-3})\lambda^2 + (1.0064)\lambda - (194.84) \quad (2)$$

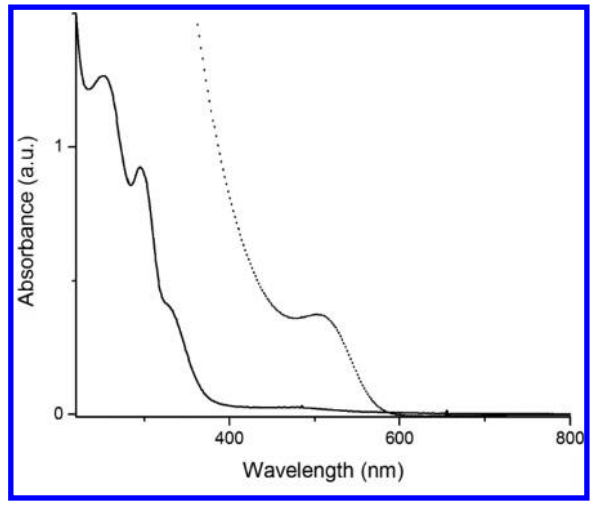

Figure 1. Aqueous UV−vis absorption spectra of the salt *cis*-[Ru(NO)(4-ampy)(bpy)$_2$](PF$_6$)$_3$ (1.0×10^{-4} M; solid line) and of MPA-CdTe QDs (∼1.0×10^{-5} M; dashed line) in aqueous solutions (pH 6.0).

PL quantum yields (Φ_{PL}) for the MPA-CdTe QDs were determined by comparison to a known reference fluorophore. Different absorbances of each compound at excitation wavelength under 0.1 (to prevent inner filter effect) were measured and the quantum yield was calculated from the plot of absorbance versus integrated fluorescence intensities using the cited equation.[31] A Φ_{PL} value of 0.10 was determined.

When the PL from the MPA-CdTe QDs was recorded in the presence of different micromolar concentrations of Ru−NO added to the solution, it was noted that the PL intensity was quenched (Figure 2) and a slight red shift of the PL λ_{max} was observed. This red shift was more pronounced at higher values of [Ru−NO] (SI Figure S-2). Notably, there is little or no overlap of the QD emission band and the absorption spectrum of Ru−NO; thus a mechanism *other than* Förster resonance energy transfer (FRET) must be responsible for such

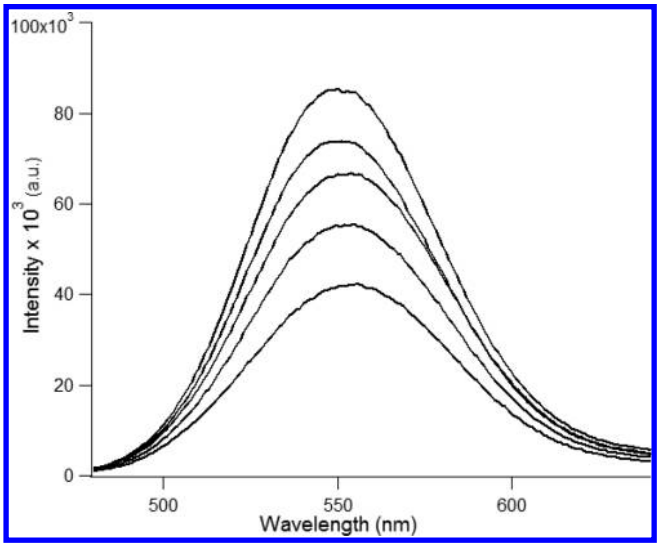

Figure 2. Quenching of the PL from MPA-CdTe QDSs in aqueous solution (5.5×10^{-6} M) by different concentrations of *cis*-[Ru(NO)(4-ampy)(bpy)$_2$]$^{3+}$ in water solution (pH 5.5). Spectra correspond to 0−20.6×10^{-6} M Ru−NO, respectively (λ_{ex} = 460 nm).

dx.doi.org/10.1021/jp5111218 | J. Phys. Chem. A 2014, 118, 12184−12191

quenching, a likely possibility being a charge transfer mechanism (see later discussion).

For low concentrations of added Ru−NO (0−2.5 μM) the Stern−Volmer (I_0/I vs [Q]) plot was roughly linear (SI Figure S-3), and the same result was observed when higher concentrations were added (Figure 3), but at higher

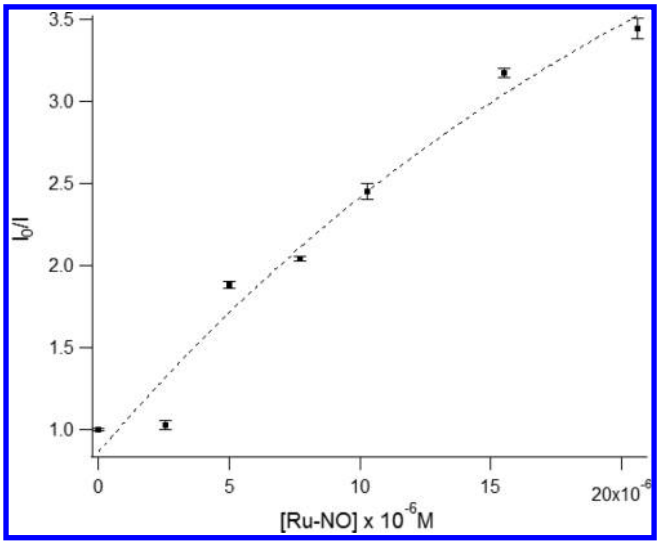

Figure 3. Stern−Volmer (I_0/I vs [Q]) plot for the data reported in Figure 2 for quenching of the MPA-CdTe QD PL (5.5 × 10^{-6} M) by different concentrations of Ru−NO: 0, 2.5 × 10^{-6}, 5.0 × 10^{-6}, 7.7 × 10^{-6}, 10.3 × 10^{-6}, 15.5 × 10^{-6}, and 20.6 × 10^{-6} M.

concentrations such plots are curved (Figure 3) suggesting saturation of the quenching process. Nonlinear behavior of this type has been attributed in other QD systems to the operation of both static and dynamic quenching.[27] For example, different plots were seen for FRET quenching of water-soluble CdSe/ZnS core/shell quantum dots by the *trans*-Cr(cyclam)(NO)$_2^+$ (CrONO), and this was attributed to the formation of electrostatic assemblies of the CrONO cations on the anionic QD surface.[8,9] For electron transfer, close contact between the two redox centers is required.[27,30,32] One possibility would be conjugation of the anionic MPA-CdTe QDs with the tricationic Ru−NO either by electrostatic attraction or by covalent linking between the two chromophores. The enhanced PL quenching with increasing [Ru−NO] would occur by progressive association of the quenchers onto the QD surface.[31] With regard to the red shift in the PL λ_{max} with increasing [Ru−NO], the relative broad absorption spectrum of the MPA-CdTe QD sample suggests a size distribution with a corresponding distribution of quenching rates. It has been shown in other cases that smaller QDs are quenched more rapidly,[27] and similar behavior in the present case may explain the shift in the PL band to longer wavelengths in the partially quenched solutions.[32]

The nature of the Ru−NO interaction with MPA-CdTe QDs was probed by electrophoresis using agarose gels according to a published procedure[28] with some modifications. The electrophoretic mobility of the MPA-CdTe QDs, of Ru−NO, and of the QD···Ru−NO conjugate should be dependent on the charge of the species. For the applied negative potential, the cationic Ru−NO species should migrate toward the negatively charged electrode (Figure 4, line 5) while the anionic MPA-CdTe QDs should migrate toward the positive electrode as

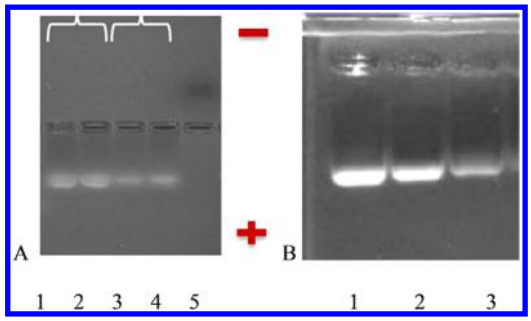

Figure 4. Mobility and luminescence intensity of the respective electrophoresis bands formed from mixtures of MPA-CdTe QDs (3.5 × 10^{-6} M) and different Ru−NO concentrations after being subjected to electrophoresis in agarose gel at 90 V for 20 min (30% glycerin (v/v)). (A) MPA-CdTe (lanes 1 and 2); MPA-CdTe and Ru-NO (1.4 × 10^{-3} M; lanes 3 and 4); and Ru-NO (2.5 × 10^{-3} M) only (lane 5). (B) MPA-CdTe QDs (lane 1); mixtures of MPA-CdTe QDs and Ru−NO in the proportions 1:5 (lane 2) and 1:10 (lane 3). The position of the wells and direction of the compounds migration are noted.

seen. The question remains whether the conjugated species are anionic or cationic. In this context, Figure 4B shows that mobility of the QD···Ru−NO conjugate slightly decreases in comparison to QD alone, probably due the increase of molecular weight and lower surface charge. The emission band intensity also decreases (Figure 4B, presumably as the result of quenching by Ru−NO migrating together with the thiol-modified quantum dot, supporting the formation of the proposed conjugate). Nonetheless, given the direction of migration, it appears that the conjugates formed remain anionic.

Figure 5 shows the PL decays for a solution of the MPA-CdTe QDs and for an analogous solution containing Ru−NO

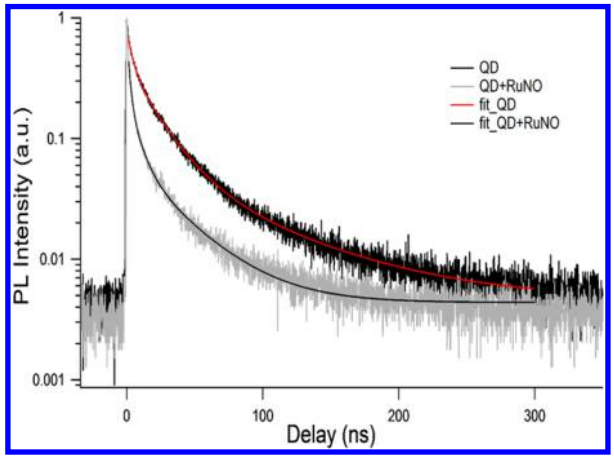

Figure 5. Luminescence decay curves measured for aqueous solutions of the free MPA-CdTe QDs (2.2 × 10^{-5} M) and for analogous solutions also containing Ru−NO (7.0 × 10^{-6} M), λ_{exc} = 400 nm.

(7.0 × 10^{-6} M). Both curves were fitted to a three-exponential function. Analysis of the temporal emission from the former solution gave τ_1 = 3.7 ± 0.1 ns, τ_2 = 20.7 ± 0.1 ns, and τ_3 = 74 ± 2.0 ns with the respective amplitudes and standard deviation 0.51, 0.42, and 0.07 (±0.01), while that for the solution containing Ru−NO gave τ_1 = 1.8 ± 0.1 ns, τ_2 = 7.5 ± 0.3 ns, and τ_3 = 35 ± 1.0 ns with the corresponding amplitudes of 0.68, 0.24, and 0.08 (±0.01). The resulted lifetime average were 15.8

dx.doi.org/10.1021/jp5111218 | J. Phys. Chem. A 2014, 118, 12184−12191

± 0.1 ns for the QDs solution only and 5.8 ± 0.2 ns for the mixture solution.

Clearly the ruthenium complex has a strong effect on the PL, decreasing the lifetimes of all three decay components. The shorter PL lifetimes with added Ru−NO are consistent with the quenching process from Ru−NO moieties on the QD surface competing with the native radiative and nonradiative deactivation of the QDs.[33]

Visible range TA spectra observed upon ultrafast excitation at 400 nm for solutions of the MPA-CdTe QDs and for analogous solutions also containing Ru−NO (2.5×10^{-6} M) are shown in SI Figure S-4. Notably, there was no difference in position and appearance of the bleached band between the TA spectra with only the QDs and those with added Ru−NO. Both sets of spectra show transient bleaching of the QD 1S band centered at about 520 nm occurring within ∼1 ps. The principal difference is that, for the QD···Ru−NO conjugates, the decay of this transient bleaching has progressed further for the longest (500 ps) of the delay times shown (SI Figure S-4, bottom). This difference is much more evident when one examines the temporal transient bleaches at 520 nm as a function of the time delay between the excitation and monitoring pulses (Figure 6). The rise of the transient bleach of the QD 1S absorption band occurs for both systems over approximately 1 ps (Figure 6, bottom), and there is little difference in the decay of this bleach over the first ∼50 ps). On a longer time scale (>100 ps), the presence of Ru−NO leads to a faster depletion of the 1S excited state. Thus, the rate constant for charge transfer would appear to fall in the range of 10^9−10^{10} s^{-1}.

Photochemical Experiments. In order to test whether Ru−NO quenching of the QD PL is coupled to photosensitized NO release, solutions of the QD···Ru−NO conjugate were irradiated at λ_{irr} 532 nm. The chronoamperogram recorded by the NO sensor (Figure 7) clearly demonstrated the release of NO. In contrast, analogous 532 nm irradiation of a solution containing only Ru−NO gave very little nitric oxide release, as expected given the very low absorption of this species at this wavelength (Figure 1).

NO release studies carried out using the NOA showed more detailed results. A solution of Ru−NO (5.7×10^{-5} M) in 10 mM citric buffer was irradiated with a green light emitting diodes (LEDs; 525−550 nm light at 20 mW) for 30 s with a long-pass filter to avoid shorter wavelengths. The same procedure was done after adding 100 μL of MPA-CdTe QDs (stock solution, ∼0.3 abs).

The enhancement of the measured NO release was >8.0 fold higher for solutions containing QDs when compared to Ru−NO solution alone (Figure 8). Analogous enhancements of NO release were also seen for longer irradiation times (Figure 9).

The product of the intensity of light absorbed (I_a) and the irradiation time gives the einsteins of light absorbed by a sample for any time interval. Plots of the moles of NO released as the result of the excitation interval vs this value (Figure 9) are linear with the slopes equaling the quantum yields for NO release. In this manner quantum yields for NO release (Φ_{NO}) from a solution of Ru−NO alone and from a solution containing both Ru−NO and the MPA-CdTe QDs (∼2×10^{-7} M) were determined to be 0.018 and 0.051, respectively. These results confirm that the QDs interact with Ru−NO and that they can be used as antennae for NO photogeneration since the CdTe—Ru−NO mixture showed a higher NO release (8-fold) when compared to Ru−NO solution only. The enhanced NO release can be attributed to the much greater

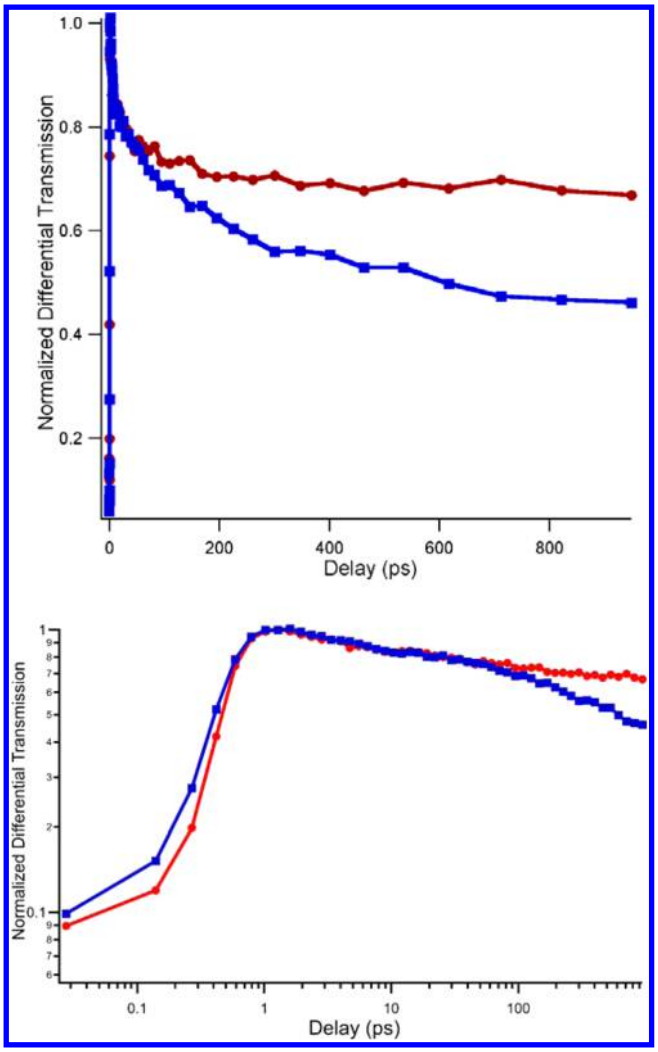

Figure 6. Top: Normalized transient differential transmission showing the bleach of the 1S QD absorption band at 520 nm as a function of delay time after ultrafast excitation with 400 nm light at 20 μJ cm^{-2} (pulse width ∼ 140 fs). Red line (round dots): MPA-CdTe QDs in aqueous solution. Blue line (square dots): MPA-CdTe QDs in aqueous solution plus plus Ru−NO (2.5×10^{-6} M) after analogous ultrafast excitation. Note the fast rise time (∼1 ps) of the transient bleaching following excitation. Bottom: The same data as a log/log plot to emphasize the changes in the first 100 ps after excitation.

absorbance of the QD containing solutions as well as to the higher quantum yield for NO release.

Notably, the mixing of purified MPA-CdTe QDs with Ru−NO in aqueous or buffer solution generates an electronic spectrum with features different from that of either of the starting species, principally the appearance of a new band at 457 nm (Figure 10). This result supports the formation of ground state complex between QDs and Ru−NO, possibly a charge transfer complex.[31,32] A similar electronic spectrum was obtained when 4-mercaptopropionic acid was added to an aqueous solution of *cis*-$[Ru(bpy)_2(4\text{-ampy})NO](PF_6)_3$ (pH = 5.5; SI Figure S-5). We attribute this spectral change to the formation of *S*-nitrosothiol adduct as compared to a similar process involving a nitrosyl−ruthenium complex in the presence of thiol ligand.[33] On the basis of this, we can infer that MPA-capped quantum dots may be best represented as having MPA bonding variously at the carboxylate and at the thiol, as described in Scheme 1.

dx.doi.org/10.1021/jp5111218 | J. Phys. Chem. A 2014, 118, 12184−12191

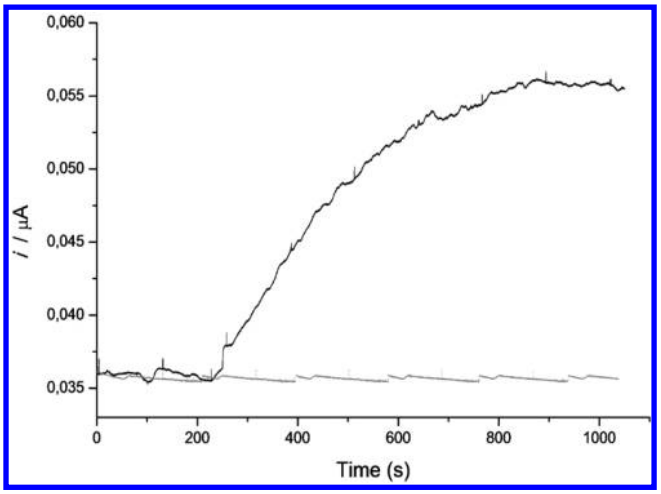

Figure 7. Chronoamperogram of NO delivery by photolysis (λ_{irr} = 532 nm). Gray line: Ru−NO (1.0×10^{-4} M) only. Black line: Ru−NO plus MPA-CdTe QDs (2 mg/3 mL), in aqueous solution (pH 5.5). The excitation was begun at ∼200 s.

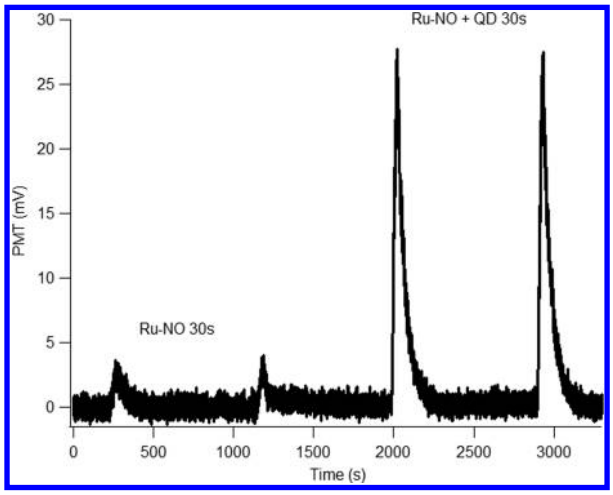

Figure 8. NO release detected by the NOA from a solution of Ru−NO before and after adding MPA-CdTe QDs. Each experiment measures the NO released upon 30 s irradiation with the green LED ($\lambda_{ex\ max}$ = 530 nm) in citric buffer solution, pH 3.6.

It is known that QDs can generate reactive oxygen species (ROS) such as singlet oxygen and superoxide during photolysis.[34] Some studies have reported free radicals production while others did not. ROS production was evaluated by photolysis of MPA-CdTe QDs in aqueous solution followed by EPR analysis using 4-hydroxy-2,2,6,6-tetramethylpiperidinyloxy (TEMPOL), which exhibits a well-known action as a scavenger of certain oxygen radicals, particularly superoxide anion.[35] The solution containing TEMPOL displayed an EPR signal that decreased slowly upon photolysis at 532 nm in aerobic aqueous solution containing the MPA-QDs (SI Figure S-6). EPR signal decreases were not observed when superoxide dismutase, a known superoxide scavenger, was also added to the analogous solutions during irradiation at 532 nm. These data indicate that a small amount of superoxide may be generated simultaneously with photosensitization of NO release upon irradiation of the MPA-CdTe QD···Ru−NO conjugates.

The acute toxicities of the CdTe QDs, Ru−NO and the conjugate between these two were evaluated using a murine melanoma cell line (B16F10). After 24 h pre-incubation, the

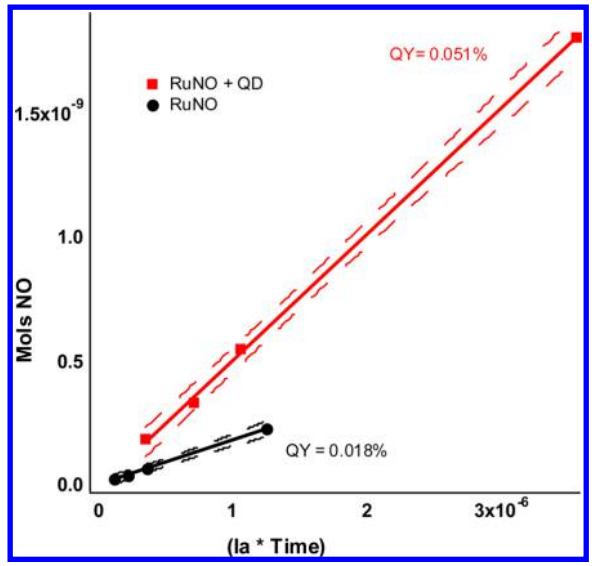

Figure 9. Plot of moles of NO released vs I_a × time (photons absorbed) when irradiated at 530 nm: squares, Ru−NO + QDs; dots, Ru−NO alone; dashed lines, 95% confidence intervals.

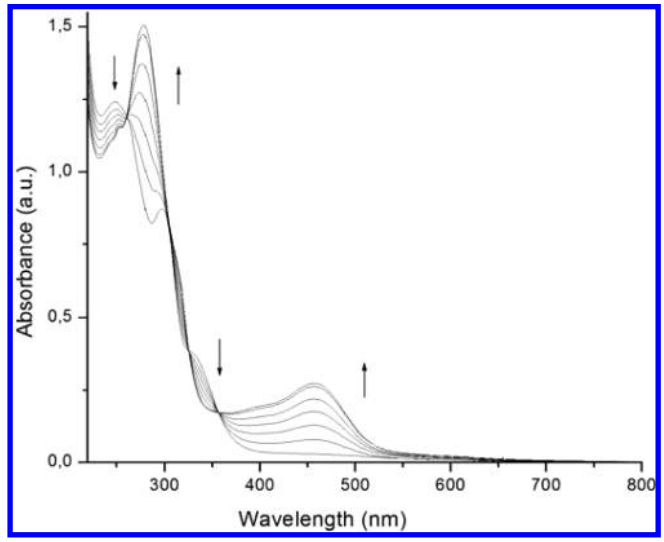

Figure 10. Absorption spectrum of Ru−NO (5.2×10^{-5} M) in the presence of different concentrations of MPA-CdTe QDs (0, 1.4×10^{-8}, 2.8×10^{-8}, 4.2×10^{-8}, 5.5×10^{-8}, 6.9×10^{-8}, and 8.2×10^{-8} M).

cells were exposed with serial concentrations (up to 2 x 10^{-3} M) of CdTe QDs and Ru−NO separately and of the MPA-CdTe QD···Ru−NO conjugate. Cells without any of these compounds added were used as the controls. The B16F10 cell proliferation was assessed using the MTT colorimetric assay. No toxicity was observed at these concentrations for the QD's or Ru−NO or for the MPA-CdTe QD···Ru−NO conjugate. Analysis of confocal images showed incorporation of QD-MP···Ru−NO^+ (S-) into the cells (SI Figure S-9). Analysis of confocal images showed incorporation of QD-MPA···Ru−NO^+ (S-) into the cells (SI Figure S-7).

SUMMARY

These results suggest that charge transfer from the excited CdTe QDs to the Ru−NO moiety is the mechanism for the photosensitization of NO release and the interaction between

dx.doi.org/10.1021/jp5111218 | J. Phys. Chem. A 2014, 118, 12184−12191

Scheme 1. Possible Surface Reaction of MPA-CdTe QDs with Ru−NO

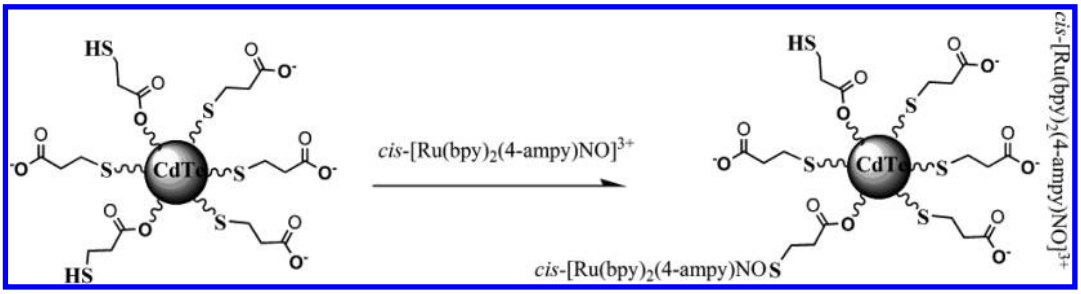

the species is a combination of both static and dynamic processes. FRET is unlikely given that there is no overlap between the absorption spectrum of Ru−NO and the emission spectrum of the QD. A substantial enhancement of NO release was obtained at longer wavelength excitation owing to the antenna effect of the QD exciton peak (λ_{max} = 503 nm). This system shows promising potential as NO photoinduced delivery. Further experiments using this system in physiologic pH and different QDs size will be discussed later in a subsequent work.

■ ASSOCIATED CONTENT

Supporting Information

Figures showing absroption and PL spectra, quenching of PL, and transient diffrerential transmission spectra of MPA-CdTe QDs, absorption spectra in the UV−vis region, EPR of TEMPOL after light irradiation, and an image of B16-F10 cells incubated 24 h with QDs. This material is available free of charge via the Internet at http://pubs.acs.org.

■ AUTHOR INFORMATION

Corresponding Authors

*(R.S.d.S.) E-mail: silva@usp.br.

*(P.C.F.) E-mail: ford@chem.ucsb.edu.

Notes

The authors declare no competing financial interest.

■ ACKNOWLEDGMENTS

This research was supported by CNPq, FAPESP, NAP PHOTOCHEM, and a U.S. National Science Foundation grant to P.C.F. (CHE-1058794). We thank Meredith Roberts from UCSB Department of Chemistry and Biochemistry for her help on NOA training.

■ REFERENCES

(1) Chaudhuri, R. G.; Paria, S. Core/Shell Nanoparticles: Classes, Properties, Synthesis Mechanisms, Characterization, and Applications. *Chem. Rev.* **2012**, *112*, 2373−2433.

(2) Sarikaya, M.; Tamerler, C.; Jen, A. K.-Y; Schulten, K.; Baneyx, F. Molecular Biomimetics: Nanotechnology through Biology. *Nat. Mater.* **2003**, *2*, 577−585.

(3) Gill, R.; Zayats, M.; Willner, I. Semiconductor Quantum Dots for Bioanalysis. *Angew. Chem. Int. Ed.* **2008**, *47*, 7602−7625.

(4) Sykora, M.; Petruska, M. A.; Alstrum-Acevedo, J.; Bezel, I.; Meyer, T. J.; Klimov, V. I. Photoinduced Charge Transfer between CdSe Nanocrystal Quantum Dots and Ru-Polypyridine Complexes. *J. Am. Chem. Soc.* **2006**, *128*, 9984−9985.

(5) Kamat, P. V. Quantum Dot Solar Cells. The Next Big Thing in Photovoltaics. *J. Phys. Chem. Lett.* **2013**, *4*, 908−918.

(6) Hines, D. A.; Kamat, P. V. Recent Advances in Quantum Dot Surface Chemistry. *ACS Appl. Mater. Interfaces* **2014**, *6*, 3041−3057.

(7) Yaghini, E.; Seifalian, A. M.; MacRobert, A. J. Quantum Dots and Their Potential Biomedical Applications in Photosensitization for Photodynamic Therapy. *Nanomedicine (London, U. K.)*. **2009**, *4*, 353−363.

(8) Neuman, D.; Ostrowski, A. D.; Mikhailovsky, A. A.; Absalonson, R. O.; Strouse, G. F.; Ford, P. C. Quantum Dot Fluorescence Quenching Pathways with Cr(III) Complexes. Photosensitized NO Production from *trans*-Cr(cyclam)$(ONO)_2^+$. *J. Am. Chem. Soc.* **2008**, *130*, 168−175.

(9) Burks, P. T.; Ostrowski, A. D.; Mikhailovsky, A. A.; Chan, E. M.; Wagenknecht, P. S.; Ford, P. C. Quantum Dot Photoluminescence Quenching by Cr(III) Complexes. Photosensitized Reactions and Evidence for a FRET Mechanism. *J. Am. Chem. Soc.* **2012**, *134*, 13266−13275.

(10) Shibu, E. S.; Ono, K.; Sugino, S.; Nishioka, A.; Yasuda, A.; Shigeri, Y.; Wakida, S.; Sawada, M.; Biju, V. Photouncaging Nanoparticles for MRI and Fluorescence Imaging in Vitro and in Vivo. *ACS Nano* **2013**, *7*, 9851−9859.

(11) Carneiro, Z. A.; et al. Photocytotoxic Activity of a Nitrosyl Phthalocyanine Ruthenium Complex—A System Capable of Producing Nitric Oxide and Singlet Oxygen. *J. Inorg. Biochem.* **2011**, *105*, 1035−1043.

(12) Pereira, A. C.; Ford, P. C.; da Silva, R. S.; Bendhack, L. M. Ruthenium-Nitrite Complex as Pro-drug Releases NO in a Tissue and Enzyme-Dependent Way. *Nitric Oxide* **2011**, *24*, 192−198.

(13) Ford, P. C. Photochemical Delivery of Nitric Oxide. *Nitric Oxide* **2013**, *34*, 56−64.

(14) Tfouni, E.; Truzzi, D. R.; Tavares, A.; Gomes, A. J.; Figueiredo, L. E.; Franco, D. W. Biological Activity of Ruthenium Nitrosyl Complexes. *Nitric Oxide* **2012**, *26*, 38−53.

(15) Ferezin, C. Z.; Oliveira, F. S.; Silva, R. S.; Simioni, A. R.; Tedesco, A. C.; Bendhack, L. M. The Complex *trans*-[RuCl([15]-aneN$_4$NO]$^{2+}$ induces Rat Aorta Relaxation by Ultraviolet Light Irradiation. *Nitric Oxide* **2005**, *13*, 170−175.

(16) Rose, M. J.; Mascharak, P. K. Photoactive Ruthenium Nitrosyls: Effects of Light and Potential Application as NO Donors. *Coord. Chem. Rev.* **2008**, *252*, 2093−2114.

(17) Becker, W. *Advanced time-correlated single-photon counting techniques*. Springer: Berlin, Heidelberg, New York, 2005.

(18) Klimov, V. I.; McBranch, D. W. Femtosecond High-Sensitivity, Chirp-Free Transient Absorption Spectroscopy using Kilohertz Lasers. *Opt. Lett.* **1998**, *23*, 277−279.

(19) Klimov, V. I.; Mikhailovsky, A. A.; McBranch, D. W.; Leatherdale, C. A.; Bawendi, M. G. Quantization of Multiparticle Auger Rates in Semiconductor Quantum Dots. *Science* **2000**, *287*, 1011−1013.

(20) Ershov, A. Yu.; Kucheryavyi, P. V.; Nikol'skii, A. B. Chemistry of Ruthenium Polypyridine Complexes: IX. Nitro-Nitrosyl Equilibrium in cis-[Ru(2,2-bpy)$_2$(L)NO$_2$]$^+$ Complexes. *Russ. J. Gen. Chem.* **2004**, *74*, 651−654.

(21) Sauaia, M. G.; Da Silva, R. S. The Reactivity of Nitrosyl Ruthenium Complexes containing Polypyridyl Ligands. *Transition Met. Chem.* **2003**, *28*, 254−259.

(22) Li, Y.; Jing, L.; Qiao, R.; Gao, M. Aqueous Synthesis of CdTe Nanocrystals: Progresses and Perspectives. *Chem. Commun. (Cambridge, U. K.)* **2011**, *47*, 9293−9311.

(23) Murray, C. B.; Norris, D. J.; Bawendi, M. G. Synthesis and Characterization of nearly Monodisperse CdE (E = sulfur, selenium, tellurium) Semiconductor Nanocrystallites. *J. Am. Chem. Soc.* **1993**, *115*, 8706−8715.
(24) Seixas de Melo, J. S.; Becker, R. S.; Maçanita, A. L. Photophysical Behavior of Coumarins as a Function of Substitution and Solvent: Experimental Evidence for the Existence of a Lowest Lying 1(n,π^*) State. *J. Phys. Chem.* **1994**, *98*, 6054−6058.
(25) Eaton, D. F. Reference Materials for Fluorescence Measurement. *Pure Appl. Chem.* **1988**, *60*, 1107−1114.
(26) Brouwer, A. M. Standards for Photoluminescence Quantum Yield measurements in Solution (IUPAC Technical Report). *Pure Appl. Chem.* **2011**, *83*, 2213−2228.
(27) Burks, P. T.; Ford, P. C. Quantum Dot Photosensitizers. Interactions with Transition Metal Centers. *Dalton Trans.* **2012**, *41*, 13030−13042.
(28) Wolcott, A.; Gerion, D.; Visconte, M.; Sun, J.; Schwartzberg, A.; Chen, S.; Zhang, J. Z. Silica-Coated CdTe Quantum Dots Functionalized with Thiols for Bioconjugation to IgG Proteins. *J. Phys. Chem. B* **2006**, *110*, 5779−5789.
(29) Mullaugh, K. M.; Luther, G. W., III. Spectroscopic Determination of the Size of Cadmium Sulfide Nanoparticles formed under Environmentally Relevant Conditions. *J. Environ. Monit.* **2010**, *12*, 890−897.
(30) Yu, W. W.; Qu, L.; Guo, W.; Peng, X. Experimental Determination of the Extinction Coefficient of CdTe, CdSe, and CdS Nanocrystals. *Chem. Mater.* **2003**, *15*, 2854−2860.
(31) Oh, M. H. J.; Chen, M.; Chuang, C.; Wilson, G.; Burda, C.; Winnik, M. A.; Scholes, G. D. Charge Transfer in CdSe Nanocrystal Complexes with an Electroactive Polymer. *J. Phys. Chem. C* **2013**, *117*, 18870−18884.
(32) Laferrière, M.; Galian, R. E.; Maurel, V.; Scaiano, J. C. Nonlinear Effects in the Quenching of Fluorescent Quantum Dots by Nitroxyl Free Radicals. *Chem. Commun. (Cambridge, U. K.)* **2006**, 257−259.
(33) Shi, G. H.; Shang, Z. B.; Wang, Y.; Jin, W. J.; Zhang, T. C. Fluorescence Quenching of CdSe Quantum Dots by Nitroaromatic Explosives and Their Relative Compounds. *Spectrochim. Acta, Part A* **2008**, *70*, 247−252.
(34) Tsay, J. M.; Trzoss, M.; Shi, L.; Kong, X.; Selke, M.; Jung, M. E.; Weiss, S. Singlet Oxygen Production by Peptide-Coated Quantum Dot−Photosensitizer Conjugates. *J. Am. Chem. Soc.* **2007**, *129*, 6865−6871.
(35) Laight, D. W.; Andrewsa, T. J.; Haj-Yehiab, A. I.; Carrier, M. J.; Änggarda, E. E. Microassay of Superoxide Anion Scavenging Activity in Vitro. *Environ. Toxicol. Pharmacol.* **1997**, *3*, 65−68.